Valence orbital response to pseudorotation of tetrahydrofuran: A snapshot using dual space analysis

Patrick Duffy,[1] José A. Sordo,[2] and Feng Wang[3,a)]
[1]*Chemistry Department, Kwantlen University College, Richmond Campus, 8771 Lansdowne Road, Richmond, British Columbia V6X 3V8, Canada*
[2]*Laboratorio de Quimica Computacional, Facultad de Quimica, Universidad de Oviedo, C/Julian Claveria 8, 33006 Oviedo, Principado de Asturias, Spain*
[3]*Centre for Molecular Simulation, Swinburne University of Technology, P.O. Box 218, Hawthorn, Melbourne, Victoria 3122, Australia*

(Received 20 November 2007; accepted 8 January 2008; published online 26 March 2008)

The pseudorotation of tetrahydrofuran (THF) (C_4H_8O) has been studied using density functional theory, with respect to the valence orbital responses to the ionization potentials and to orbital electron and momentum distributions. Three conformations of THF, the global minimum structure C_s, local minimum structure C_2, and a transition state structure C_1, which are characteristic configurations on the potential energy surface, are examined using the SAOP/et-pVQZ//B3LYP/6-311++G** models with the aforementioned dual space analysis. It is noted in the ionization energy spectra that the minimum structures C_s and C_2 are not directly connected by pseudorotation, but through the transition state structure C_1. As a result, some orbitals of the C_s conformer are able to "correlate" to orbitals of the C_2 conformer without a strict symmetry constraint, i.e., orbital 7a′ of the C_s conformer is correlated to orbital 5*b* of the C_2 conformer. It is also noted that although the valence orbital ionization potentials are not significantly altered by the pseudorotation of THF, their spectra (mainly due to excitation) are quite different indeed. Detailed orbital analysis based on dual space analysis is given. The valence orbital behavior of the conformations is orbital dependent. It can be approximately divided into three groups: the "signature group" is associated with orbitals experiencing significant changes. The frontier orbitals are in this group. The "nearly identical group" includes orbitals without apparent changes across the conformations. Most of the orbitals showing a certain degree of distortion during the pseudorotation process belong to the third group. The present study demonstrates that a comprehensive understanding of the pseudorotation of THF and its dynamics requires multidimensional information and that the information gained from momentum space is complementary to that from the more familiar coordinate space. © *2008 American Institute of Physics*. [DOI: 10.1063/1.2838852]

I. INTRODUCTION

Conformational analysis is a subject of paramount importance when a better understanding of the origin of a great variety of physical, chemical, and biological processes is desired. For example, conformational analysis allowed Kilpatrick *et al.* to explain the anomalously high entropy of cyclopentane in terms of a conformational phenomenon denoted as pseudorotation.[1] As another example, the determination of torsional potentials around the C–C single bond in 1,3-butadiene and conjugated systems still remains a very active research area.[2] Indeed, understanding the equilibrium between the *s-trans* and *s-cis* conformers is an important factor when rationalizing the mechanism involved in fundamental reactions in organic chemistry such as cheletropic and Diels-Alder cycloadditions.[3] As a biological illustration of the importance of conformational analysis one could mention that experimental and theoretical conformational studies on biomolecules, such as amino acids, have been the focus of a great deal of attention in recent literature because of their biological significance as building blocks of peptides and proteins.[4]

In this brief discussion of the applications of conformational analysis in different fields we should also stress the importance of conformational preferences in pharmacology. The analysis becomes crucial when planning the synthesis of molecules exhibiting biological activity to be employed as potential drugs in the therapeutic treatments of diseases such as acquired immune deficiency syndrome (AIDS).[5]

Since geometrical changes and energy variations accompanying conformational motions for a given molecule can be rather small, determination of the most stable structure can become an extraordinarily difficult task.[6–8] This is indeed the case for tetrahydrofuran (THF), a heterocyclic five-membered ring which can be regarded as a prototypical structural unit of, say, carbohydrate and biological molecules.[9] Thus, for example, a derivative of THF, azidothymine, is commonly recognized as the first anti-AIDS drug used in antiviral chemotherapy and prophylaxis in the United States.[10]

THF is not a planar molecule in the gas phase but ex-

a)Author to whom correspondence should be addressed. Electronic mail: fwang@swin.edu.au.

 © 2008 American Institute of Physics

Downloaded 22 Jun 2009 to 136.186.1.191. Redistribution subject to AIP license or copyright; see http://jcp.aip.org/jcp/copyright.jsp

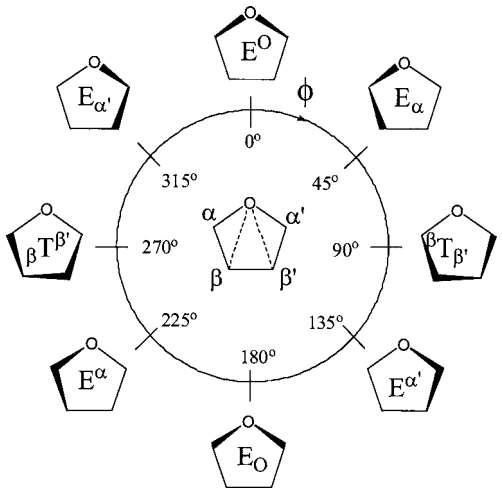

FIG. 1. Pseudorotation of THF. The principal a axis coincides with the C_2 axis, and the b axis is within the plane of the nonpuckered ring (center). Envelope (E) conformations are characterized by coplanarity of four adjacent ring atoms and twisted conformations (T) by coplanarity of three adjacent ring atoms and the midpoint between the opposite bonds. The indices refer to ring atoms above (superscript) or below (subscript) the ab plane.

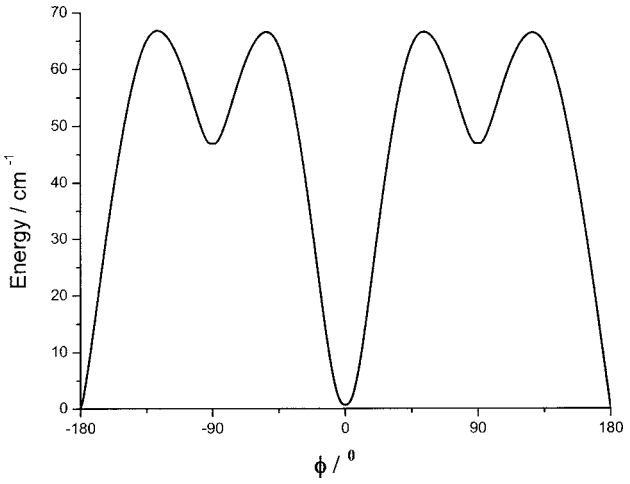

FIG. 2. *Ab initio* potential function for pseudorotation in THF (see text for details).

hibits pesudorotation,[1] that is, a vibrational motion in which the molecule consecutively transforms into a number of energetically quite similar structures: envelope like $[E^o(C_s)$, $E_{\alpha}(C_1)$, $E^{\alpha'}(C_1)$, $E_o(C_s)$, $E^{\alpha}(C_1)$, $E_{\alpha'}(C_1)]$ and twisted $[{}^{\beta}T_{\beta'}(C_2)$, ${}_{\beta}T^{\beta'}(C_2)]$ conformations (see Fig. 1). Pseudorotation allows the THF to invert ($E^o \rightarrow E_o$ in Fig. 1) without passing through the higher-energy planar structure by means of a ring-puckering motion.

Over the last four decades, pseudorotation of THF has been investigated[6,8] and a number of experimental structural studies on THF, mostly using infrared and microwave spectroscopy, have been published. However, a general consensus about the minimum energy structure of this molecule has not been achieved yet. While Engerholm *et al.*[12] and Meyer *et al.*[13] proposed a potential function for pseudorotation in THF with four equivalent minima $[E_{\alpha}(C_1)$, $E^{\alpha'}(C_1)$, $E^{\alpha}(C_1)$, $E_{\alpha'}(C_1)]$, Mamleev *et al.*[14] and Melnik *et al.*[8] reported that the twisted ${}^{\beta}T_{\beta'}(C_2)$ and ${}_{\beta}T^{\beta'}(C_2)$ conformations represent two equivalent global minima structures for THF. The previous work illustrates the enormous difficulties associated with the conformational analysis of the THF. Indeed, after about 40 years of both theoretical and experimental research,[6,8,12–14] the question of the equilibrium geometry of THF has not been resolved.

From the theoretical point of view, several works,[8,9,15,16] employing MP2 or density functional theory (DFT) (B3LYP) methodologies, with Pople's or Dunning's standard basis sets,[11] predicted the twisted conformations to be the global minima on the potential energy surface (PES). More recently, a theoretical study, in which geometry optimizations were carried out at the MP2/aug-cc-pVTZ level, has been published.[7] The energy predictions were estimated through CCSD(T)/cc-pVTZ single-point calculations, extrapolated to the complete basis set (CBS) limit[17] by means of a series of MP2/cc-pVXZ ($X=T,Q,5$) calculations and consideration of anharmonic contributions [CCSD(T)/cc-pVTZ//MP2/cc-pVTZ+CBS(MP2-TQ5)+ZPE(anharmonic) level]. Such a high level *ab initio* methodology predicted a PES like the one presented in Fig. 2, with $E^o(C_s)$ and $E_o(C_s)$ being global minima structures, ${}^{\beta}T_{\beta'}(C_2)$ and ${}_{\beta}T^{\beta'}(C_2)$ local minima structures, and $E_{\alpha}(C_1)$, $E^{\alpha'}(C_1)$, $E^{\alpha}(C_1)$, $E_{\alpha'}(C_1)$ representing transition structures connecting the different minima. This theoretical prediction differs from all the previously proposed PESs.[6,8,9,12–16] Rayón and Sordo[7] stressed the fact that since the energy differences between the involved structures are so small, special care should be exercised when choosing an appropriate computational level to deal with the extremely difficult conformational problem of pseudorotation in THF.

Because of the complexities and subtleties associated with obtaining and analyzing position space (energy) information,[7] it has been shown to be beneficial to examine the problem in a different way. To that end, information from momentum space [momentum distributions or (MDs)] can be very valuable. Yang *et al.*[18] employed this approach and focused on the identification of symmetries of the highest occupied molecular orbital (HOMO) of the C_2 and C_s conformers of THF by using dual space analysis (DSA).[19] They found the most populated conformer of this molecule in the gas phase under the experimental conditions to be the C_s conformer, in agreement with the high level *ab initio* predictions.[7]

In the present work, we extend previous studies on THF by reporting the results of comprehensive quantum mechanics (QM) orbital MD simulations of the individual outer valence orbitals of this molecule. As some of the orbital MDs of THF are not yet fully resolved by experiment,[18] the present study will provide additional information that might well help to complement the experimental work. In addition, various QM models will be employed in order to assess their performance as well as the suitability of the different approximations on which such models are based.

The final stage of any conformational study should involve a dynamical treatment which can only be accomplished when the structures appearing on the PES are well

Downloaded 22 Jun 2009 to 136.186.1.191. Redistribution subject to AIP license or copyright; see http://jcp.aip.org/jcp/copyright.jsp

characterized. The present study contributes to that goal by employing an appropriate theoretical tool: DSA.[19]

II. METHODS AND COMPUTATIONAL DETAILS

In the present study, geometries of the C_s, C_1, and C_2 structures involved in pseudorotation of THF were obtained at the B3LYP/6-311++G** level,[18] using the GAUSSIAN03 (Ref. 20) packages of programs. Hessian calculations showed that both C_s and C_2 structures have all positive frequencies, suggesting that they could be characterized as minimum configurations on the PES.[7,18] The C_1 conformation resulted in negative frequencies,[18] indicating that it is a transition structure connecting the C_s and C_2 minima structures. The 6-311++G** basis set was chosen because it appears to give good geometric properties in combination with DFT models, whereas reduced bases, such as Pople's standard 6-31G* basis set, seem not to be appropriate in some cases.[21] A recent DFT conformation study on methyl tetrahydrofuran-2-carboxylate supports this, revealing that a number of DFT functionals available in the GAUSSIAN03 computational package, such as B1LYP, B3LYP, B3P86, B3PW91, B98, BHandHLYP, MPW1PW91, and PBE1PBE, do not provide an unambiguous PES when used with the 6-31G* basis set, but give a uniform picture when paired with the cc-pVTZ basis set.[21] This result is not surprising as a number of factors, such as the DFT functionals, basis sets (Gaussian or Slater), the combination of the DFT functional and the basis sets, as well as the properties studied and the molecules themselves, affect the results.[22,23]

DSA (Ref. 19) has been employed in the present conformational study. This type of analysis, providing a combined method for processing information from coordinate and momentum spaces such as energies and orbital MDs, has proven capable of providing a unique, novel, and comprehensive means to study conformers unambiguously.[2,4(b),18,24–28]

Vertical ionization energies (approximated using negative orbital energies) and orbital MDs in the outer valence space ($IP_i < 20$ eV) of the THF conformers were obtained by using QM models from DFT that employ two different functionals: (a) the B3LYP functional[29,30] and (b) the statistical average of orbital potential (SAOP) functional.[31,32] B3LYP was chosen because it is one of the most popular DFT functionals, providing good results in a wide variety of problems.[11] B3LYP is a hybrid functional which includes exact exchange from Hartree-Fock theory. The SAOP functional was chosen because it was specially designed to provide a good prediction of the exchange-correlation Kohn-Sham potential in the calculation of vertical excitation energies for both the outermost occupied orbital as well as for the inner orbitals. An even-tempered (et) Slater-type orbital (STO) split-valence quadruple-zeta plus polarization (PVQZ) basis set [et-PVQZ (Ref. 33)] was employed in the DFT (SAOP) calculations of orbital energies and MDs. It has been shown recently[24] that et-STO calculations exhibit an overall good quality for the orbital density distributions in momentum space, in good agreement to the experimental electron momentum spectroscopy (EMS) measurements.

Under the Born-Oppenheimer approximation and the plane-wave impulse approximation,[34,35] the triple differential EMS cross section (momentum distribution σ_{EMS}) is proportional to the spherically averaged square of the Fourier transform of a Dyson orbital

$$\sigma_{\mathrm{EMS}} \propto \int |\langle \mathbf{p}|\psi(i)\rangle|^2 d\Omega_{\mathbf{p}}, \tag{1}$$

where $\mathbf{p}$ denotes a plane-wave spin orbital with that momentum [$\exp(-i\mathbf{pr}$] and $\psi(i)$, the Dyson orbital, is given by

$$\psi(i) = \sqrt{N} \int \int \cdots \int \Psi_f^{(N-1)}(1,2,\ldots,i-1,i+1,\ldots,N) \times \Psi_i^{(N)}(1,2,\ldots,N) dr_1 dr_2,\ldots,dr_{i-1} dr_{i+1},\ldots,dr_N, \tag{2}$$

with $1,2,\ldots,N$ representing the electronic spin and space coordinates. $\Psi_f^{(N-1)}$ and $\Psi_i^{(N)}$ are the electronic many-body wave functions for the final ion f and the target i molecular ground electronic states.

Within the so-called target Kohn-Sham approximation,[36] the renormalized Dyson orbitals $\psi_{(i)}$ can be approximated in terms of the Kohn-Sham orbitals φ_i according to

$$\psi(i) \approx \sqrt{S^{(i)}}\varphi_i, \tag{3}$$

where $S_I^{(i)}$ is a spectroscopic factor.[36]

Substitution of Eq. (3) in (1) and further application of the Dirac-Fourier transformation, $\varphi_i(\mathbf{p}) = \langle \mathbf{p}|\varphi_i(\mathbf{r})\rangle$, gives

$$\sigma_{\mathrm{EMS}} \propto S_I^{(i)} \int |\varphi_i(\mathbf{p})|^2 d\Omega_{\mathbf{p}}, \tag{4}$$

where $\varphi_i(\mathbf{p})$ is the momentum space canonical Kohn-Sham orbital.

In the present work, the Kohn-Sham orbitals were generated using SAOP/et-pVQZ//B3LYP/6-311++G** QM models in coordinate space. Then, the orbital MDs (perfect-resolution EMS cross sections) of the C_2, C_1, and C_s THF conformers were simulated using the HEMS program.[37,38] It should be noted that the momentum distributions shown in the present study are different than those shown in Ref. 18; the distributions shown in Ref. 18 incorporate experimental resolution into their calculation, thus providing a full theoretical simulation of the experiment.

III. RESULTS AND DISCUSSIONS

Ionization energy offers a quantum mechanical diagnostic for the oxidative potential of species; there is a strong correlation between a molecules' ionization potential (IP) and its ability to reduce a target molecule.[39] Table I lists the vertical IPs of the (minima) C_s and C_2 conformers in valence space, respectively, calculated using HF/aug-cc-pVTZ, SAOP/et-pVQZ, and B3LYP/et-pVQZ models. It is seen in this table that the orbital symmetries of the C_s and C_2 conformers produced using the three models are consistent for the C_s conformer, whereas the order of the $4b$ and $6a$ orbital pair (highlighted in the table) for the C_2 conformer in the HF/aug-cc-pVTZ and SAOP/et-pVQZ models are altered. This suggests that the inclusion of electron correlation energy may contribute to the exchange of the orbital pair, since

Downloaded 22 Jun 2009 to 136.186.1.191. Redistribution subject to AIP license or copyright; see http://jcp.aip.org/jcp/copyright.jsp

TABLE I. Valence ionization energies (IPs) of THF calculated using different models.

HF/aug-cc-pVTZ[a]				SAOP/et-pVQZ[a]				B3LYP/et-pVQZ[a]			
C_s Sym	ε_i (eV)	C_2 Sym	ε_i (eV)	C_s[b] Sym	ε_i (eV)	C_2 Sym	ε_i (eV)	C_s Sym	ε_i (eV)	C_2 Sym	ε_i (eV)
$12a'$	11.42	$9b$	11.10	$12a'$	10.61(9.74)	$9b$	10.30	$12a'$	7.06	$9b$	6.76
$8a''$	12.71	$11a$	12.62	$8a''$	12.21(11.52)	$11a$	11.96	$8a''$	8.82	$11a$	8.58
$11a'$	12.80	$10a$	13.01	$11a'$	12.21	$10a$	12.36	$11a'$	8.99	$10a$	9.08
$7a''$	13.34	$8b$	13.43	$7a''$	12.63(12.07)	$8b$	12.77	$7a''$	9.44	$8b$	9.62
$10a'$	13.58	$9a$	13.70	$10a'$	12.96(12.52)	$9a$	13.00	$10a'$	9.72	$9a$	9.80
$6a''$	14.82	$7b$	15.19	$6a''$	14.10(14.1)	$7b$	14.25	$6a''$	10.92	$7b$	11.11
$9a'$	15.92	$8a$	16.06	$9a'$	14.49(14.5)	$8a$	14.74	$9a'$	11.34	$8a$	11.70
$5a''$	16.71	$6b$	16.07	$5a''$	15.39(15.4)	$6b$	15.04	$5a''$	12.24	$6b$	11.88
$8a'$	18.24	$7a$	18.29	$8a'$	16.25(16.8)	$7a$	16.49	$8a'$	13.19	$7a$	13.49
$7a'$	18.55	$5b$	18.63	$7a'$	16.57	$5b$	16.78	$7a'$	13.50	$5b$	13.79
$4a''$	21.81	$4b$	22.01	$4a''$	18.91(19.3[c])	$6a$	18.90	$4a''$	16.08	$6a$	16.08
$6a'$	22.37	$6a$	22.02	$6a'$	19.16	$4b$	19.14	$6a'$	16.32	$4b$	16.35
$3a''$	26.90	$3b$	26.96	$3a''$	22.49	$3b$	22.72	$3a''$	19.90	$3b$	20.16
$5a'$	28.64	$5a$	28.91	$5a'$	23.71	$5a$	23.87	$5a'$	21.19	$5a$	21.39
$4a'$	37.40	$4a$	37.08	$4a'$	30.31	$4a$	30.60	$4a'$	27.94	$4a$	28.27

[a]B3LYP/6-311++G** geometries were used.
[b]HeI photoelectron spectrum of tetrahydrofuran from Ref. 44 are given in the parentheses.
[c]From Ref. 18 of a recent EMS measurement.

the B3LYP/et-pVQZ calculations agree with the SAOP/et-pVQZ model. The orbital energies of the pair are very close in value as 22.01 and 22.02 eV for $4b$ and $6a$, respectively, using the HF model. The energy splitting of the same orbital pair is as large as 0.24 eV when electron correlation effects are included (SAOP/et-pVQZ). It is also noted that the calculated orbital energies of the conformations are slightly different from those given in Ref. 18 using the same SAOP/et-pVTZ method based on a different set of MP2/aug-cc-pVTZ optimized geometries. Comparison with the photoelectron spectroscopy and EMS measurements shows that the energies of the frontier orbitals are slightly less accurately calculated when the THF geometry is based on the B3LYP/6-311++G** as in the present study, whereas there is an improvement in agreement of the valence orbital energies in the middle band of the valence space. Two orbitals of the C_s conformer, $8a''$ and $11a'$ are accidentally degenerate at the SAOP/et-pVQZ level, which is consistent with the experiments,[18,40] at least within the limits of experimental resolution. This orbital pair may be readily differentiated using their orbital MDs, however, due to their differing symmetries. This will be discussed in more detail below.

Although Ref. 18 produced outer valence ionization spectra of the most populated THF conformer, C_s, they did not attempt to examine how the valence orbitals of the conformations would respond to the pseudorotation of THF. This question does not have a simple answer, because (i) the energy barriers between the conformers through pseudorotation are small,[16] leading to experimental spectral congestion and (ii) the C_s and C_2 conformers of THF are not directly correlated; their association is always through the C_1 conformation as a transition state as shown in Figs. 1 and 2. An energy diagram shown in Fig. 3 associates the (occupied) orbital energies in the valence space for the C_s and C_2 conformers, through those of the C_1 transition state. As observed in Fig. 2, the three conformations are characteristic structures on the cross section of the pseudorotation potential energy surface. Although C_1 represents a transition state on the cross section, it connects the two minima structures of C_s and C_2 through pseudorotation.

The requirements for the formation of MOs for conform-

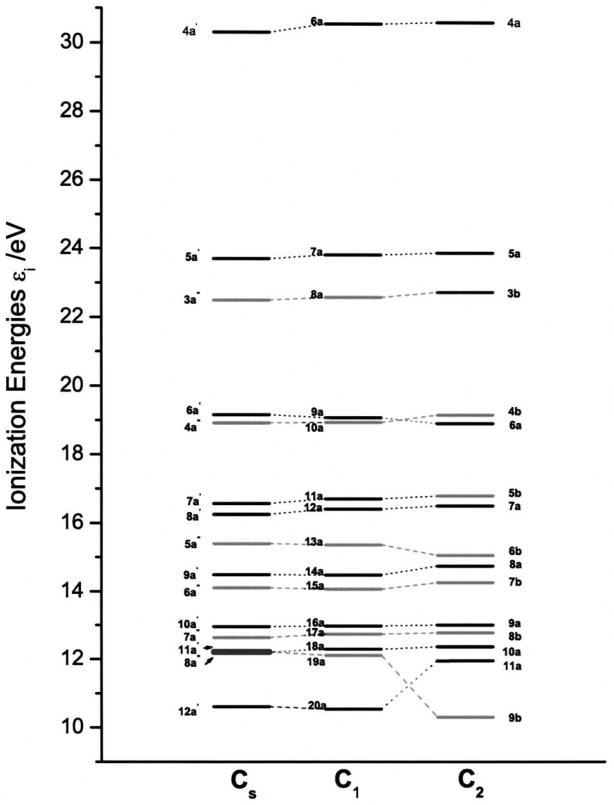

FIG. 3. Valence ionization potential energies of THF conformations: C_s (left), C_1 (middle), and C_2 (right). The energy levels in red (in color) or gray (in black and white) indicate the orbitals associated with asymmetric orbitals a'' of the C_s conformer.

Downloaded 22 Jun 2009 to 136.186.1.191. Redistribution subject to AIP license or copyright; see http://jcp.aip.org/jcp/copyright.jsp

TABLE II. Dominant contributions from atomic orbitals to valence MOs of the conformations (SAOP/et-pVQZ). (Dominant contributions with interactions stronger than 10% are shown in this table.)

MO	C_s		C_1		C_2	
set	MO	AOs	MO	AOs	MO	AOs
20	$12a'$	O(2*p*)+H(1*s*)	20*a*	O(2*p*)	9*b*	O(2*p*)+H(1*s*)
19	$8a''$	C(2*p*)+O(2*p*)+H(1*s*)	19*a*	O(2*p*)	11*a*	C(2*p*)+O(2*p*)
18	$11a'$	C(2*p*)+O(2*p*)+H(1*s*)	18*a*	H(1*s*)	10*a*	C(2*p*)+H(1*s*)
17	$7a''$	C(2*p*)+H(1*s*)	17*a*	C(2*p*)	8*b*	C(2*p*)+H(1*s*)
16	$10a'$	C(2*p*)+O(2*p*)	16*a*	C(2*p*)+O(2*p*)+H(1*s*)	9*a*	C(2*p*)+O(2*p*)+H(1*s*)
15	$6a''$	C(2*p*)+O(2*p*)+H(1*s*)	15*a*	C(2*p*)+O(2*p*)+H(1*s*)	7*b*	C(2*p*)+O(2*p*)+H(1*s*)
14	$9a'$	C(2*p*)+O(2*p*)+H(1*s*)	14*a*	C(2*p*)+O(2*p*)+H(1*s*)	8*a*	C(2*p*)+H(1*s*)
13	$5a''$	C(2*p*)+O(2*p*)+H(1*s*)	13*a*	C(2*p*)+O(2*p*)+H(1*s*)	6*b*	C(2*p*)+O(2*p*)+H(1*s*)
12	$8a'$	C(2*p*)+H(1*s*)	12*a*	O(2*p*)+H(1*s*)	7*a*	C(2*p*)+O(2*p*)+H(1*s*)
11	$7a'$	C(2*p*)+H(1*s*)	11*a*	O(2*p*)+H(1*s*)	5*b*	C(2*p*)+O(2*p*)+H(1*s*)
10	$4a''$	C(2*p*/Vir.)+O(2*p*)+H(1*s*)	10*a*[a]	C(2*p*)+O(2*s*,2*p*)	6*a*	C(2*s*,2*p*)+H(1*s*)
9	$6a'$	C(2*s*)+H(1*s*)	9*a*[a]	O(2*s*,2*p*)+H(1*s*)	4*b*	C(2*p*,Vir.)+O(2*p*)+H(1*s*)
8	$3a''$	C(2*s*)+O(2*p*)+H(1*s*)	8*a*	C(2*p*)+O(2*p*)	3*b*	C(2*s*)+O(2*p*)+H(1*s*)
7	$5a'$	C(2*s*)+H(1*s*)	7*a*	C(2*s*)	5*a*	C(2*s*,2*p*)+O(2*p*)+H(1*s*)
6	$4a'$	C(2*s*)+O(2*s*)	6*a*	O(2*s*)	4*a*	C(2*s*)+O(2*s*)

[a]Weak interactions of less than 10% contributions in these orbitals.

ers of a polyatomic molecule are energy and symmetry.[41] Correlations of the MOs among the THF conformations as a function of the pseudorotation motion angle ϕ can be represented in a diagram like Fig. 3, which is similar to the Walsh molecular orbital diagram[42] for diatomic molecules. The correlations can be obvious by their orbital shapes for diatomic molecules and polyatomic molecular configurations produced by rotations around a single bond, such as *n*-butane.[43] This may not be the case, however, for sugar puckering (pseudorotation) in molecules such as THF. The relaxation of symmetry restrictions in different point group symmetries, such as C_2 and C_s, may result in changes of point groups and changes of electronic states from, e.g., the ground state to excited or ionized states.[41] Such changes in point groups among configurations only occur in polyatomic molecules such as THF, as shown in MO set 11 of $7a'(C_s)$-$11a(C_1)$-$5b(C_2)$ (refer to Table II). The association of the $7a'$ MO of the C_s conformer and the $5b$ of the C_2 conformer indicates the changes in point groups, which is discussed in later sections.

The structures of the valence orbitals do not exhibit significant energy changes during the pseudorotation motion as shown in Fig. 3. The electronic spectra, which are produced by excitation/ionization transitions among the occupied and virtual orbitals of the conformations, however, are quite different. This is a result of the subtle differences in valence energies, electric dipoles, and orbital symmetries of the conformations and, therefore, different probabilities for various transitions of electrons in the three conformers shown. The simulated electronic spectra (density of states) of the THF conformations are given in Fig. 4. The spectra are generated using transitions to excited states from the occupied orbitals, with a Gaussian linewidth of $0.05E_h$, i.e., ~0.136 eV, based on the SAOP/et-pVQZ model calculations. As indicated earlier, similar patterns of their valence orbitals shown in Fig. 3 do not necessarily lead to similarities in their spectra, as the probabilities of transitions and their intensities will alter significantly in individual conformations. Figure 4 indeed indicates that the three conformations are different species.

Figures 2–4 show properties dominated by energetics. We now explore information revealed by orbitals of the species. All 15 symmetry correlated molecular orbital (MO) sets (based on Fig. 3) of the valence orbital MDs of the three conformations are shown in Fig. 5. The responses of valence orbital MDs to the pseudorotation is, in general, orbital dependent. These orbital MDs can be classified into three groups based on their degree of response to pseudorotation, as follows: group I orbitals (MO sets 20-18, 11, and 9 in Table II) which respond significantly to the pseudorotation motion of tetrahydrofuran, including five sets of orbital trios [colored in yellow (for color) or light gray (in black and white) in Table II]; group III orbitals (MO sets 17 and 6) of $7a''(C_s)$-$17a(C_1)$-$8b(C_2)$ and $4a'(C_s)$-$6a(C_1)$-$4a(C_2)$ exhibit

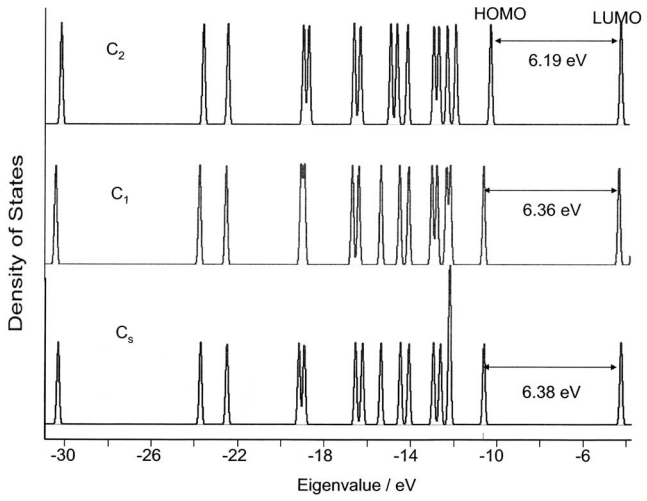

FIG. 4. Simulated electron spectra of C_s (top panel), C_1 (middle panel), and C_2 (bottom panel) conformers using SAOP/et-pVQZ. The spectral line broadening is generated using a Gaussian profile with a line width of $0.05E_h$, i.e., 0.135 eV.

Downloaded 22 Jun 2009 to 136.186.1.191. Redistribution subject to AIP license or copyright; see http://jcp.aip.org/jcp/copyright.jsp

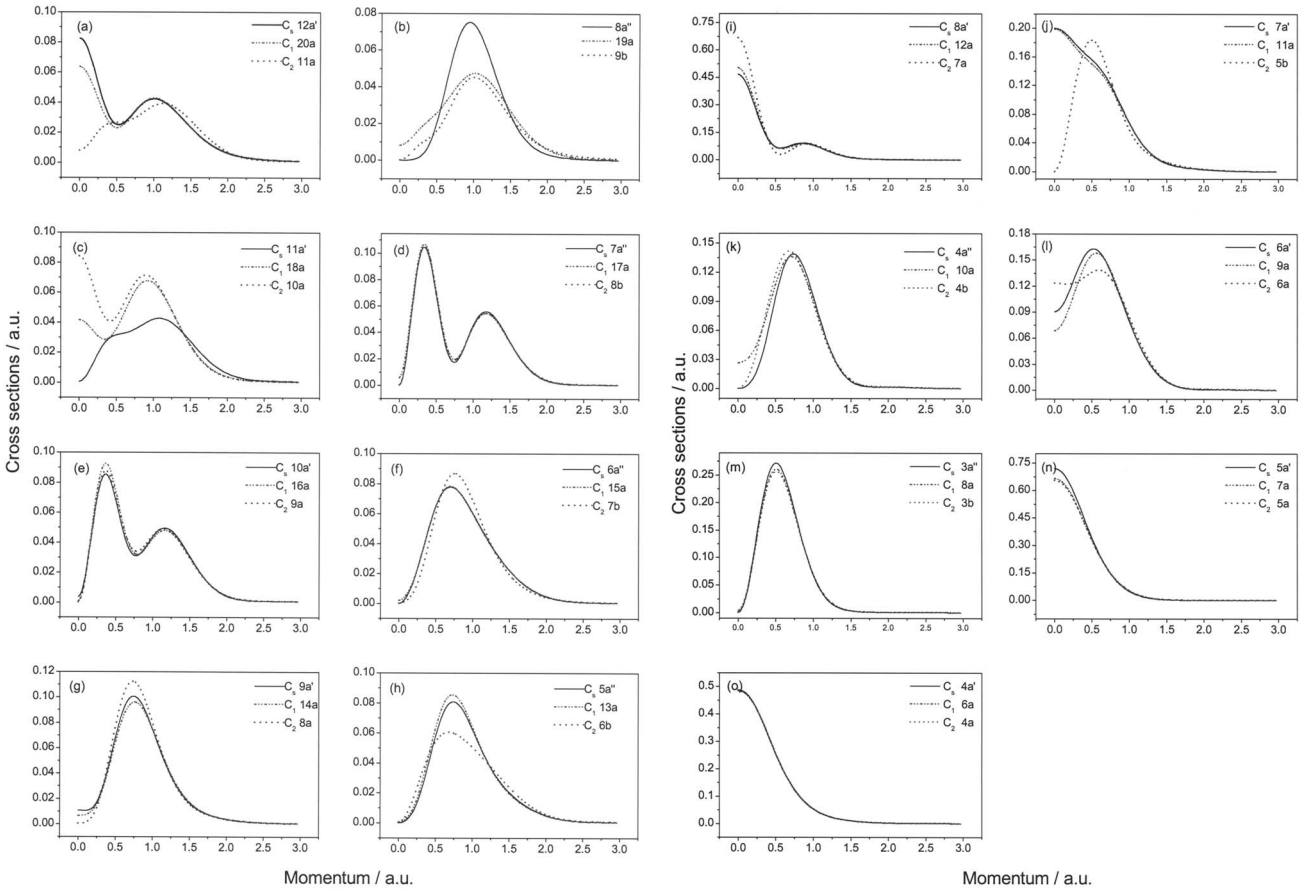

FIG. 5. All the valence orbital MDs of the C_s, C_1, and C_2 conformations of tetrahydrofuran. Associations among the valence orbital MDs of the three conformations are made according to the ionization energy diagram in Fig. 3.

almost identical orbital MDs (which are colored in dark gray in Table II); and group II orbitals (MO sets of 16-12, 10, 8-7). Orbitals in this group show a certain degree of distortion in orbital momentum distributions but no significant changes. The majority of the valence orbitals are classified as group II orbitals.

Orbitals in group II (MO sets 16-12, 10, 8-7) may be considered as a transition from group I (signature orbitals) to group III (nearly identical orbitals). Combining Fig. 5 and Table II, it is seen that the valence orbital MDs exhibit conformational similarities in pairs: the middle bond of the valence orbitals, MO sets of 15-12, exhibit similarities between C_1 and C_s conformations; whereas the inner band of valence orbitals, MO sets of 7–8 show a closer relationship between C_1 and C_2. Two MO sets, 10 and 16, show certain similarities between the C_2 and C_s conformers. The variation of pairing among the C_s, C_1, and C_2 conformations indicates that connections at various stages are possible among the conformations due to the low energy barriers of pseudorotation, which may lead to some experimental measurements to favor certain configurations depending on the experimental conditions used (such as temperature and pressure).

For the group III orbitals, which are colored in gray in Table II, MO set 17, i.e., $7a''(C_s)$-$17a(C_1)$-$8b(C_2)$ is the forth frontier orbital of the conformers in the valence space, whereas the other set of orbitals, MO set 6 ($4a'(C_s)$-$6a(C_1)$-$4a(C_2)$), is the innermost valence orbital of the THF conformations. As indicated in Figs. 3 and 5, this couple of sets of orbitals is not so sensitive to the pseudorotation motion of the THF ring. The ring puckering changes neither the orbital momentum distributions not the orbital energies very much. However, although nearly identical in momentum space and in energy across the conformations, the bonding mechanisms of the two sets of orbitals are not the same. Orbital MDs of the innermost valence orbital set 6 ($4a'(C_s)$-$6a(C_1)$-$4a(C_2)$) indicate a strong s-electron contribution because of the half bell shaped momentum distributions, whereas orbital set 17 ($7a''(C_s)$-$17a(C_1)$-$8b(C_2)$) indicates that electrons with higher angular momenta ($l \neq 0$) are involved.[44]

Table II lists the dominant atomic orbital (AO) contributions to the valence MO from the present SAOP/et-pVQZ//B3LYP/6-311++G** calculations. It demonstrates that valence orbitals are dominated by the $2s$ and $2p$ AO of the "heavy atoms" (nonhydrogen first row elements Li–Ne) as well as the $1s$ AO on hydrogen. This table also suggests certain patterns of bonding mechanisms among the configurations in which certain orbitals may be likely associated. It is noted that the AO contributions to the MO $4a'$ of the C_s conformer, MO $6a$ of the C_1 conformations, and MO $4a$ of the C_2 conformer of THF are all dominated by contributions from the $2s$ AOs of the component for the C_s and C_2 conformers, the $2s$ AO contributions to their intermost MOs, $4a'$ and $4a$, are from the associated C an O

Downloaded 22 Jun 2009 to 136.186.1.191. Redistribution subject to AIP license or copyright; see http://jcp.aip.org/jcp/copyright.jsp

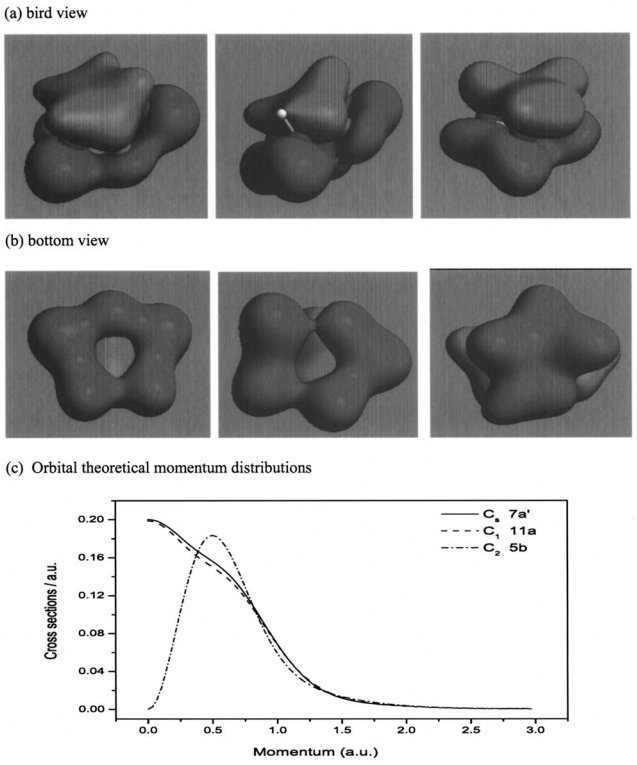

FIG. 6. Orbital similarities and differences revealed by the orbital electron density contours and orbital MDs for MO set 17 ($7a'(C_s)$-$11a(C_1)$-$5b(C_2)$).

atoms, whereas only the $2s$ AO of the O atom makes contributions to the $6a$ MO of the C_1 conformation due to its low symmetry restriction. For MO set 17 ($7a''(C_s)$-$17a(C_1)$-$8b(C_2)$), in the outer valence space on the other hand, all MOs are dominated by the $2p$ AOs. For example, the $17a$ orbital of the C_1 conformer is dominated by the carbon $2p$ AOs alone. For the higher symmetry conformers, the associated set 17 MO is dominated by the overlap of the $2p$ AO of carbon and the $1s$ AO of hydrogen; the additional symmetry restrictions present in the C_s and C_2 conformers ensure the hydrogen contribution to this orbital. However, the overlap between a $2p$ ($l=1$) AO and $1s$ ($l=0$) AOs does not change the angular momentum of the orbitals, so that the resulting molecular orbitals are unlikely to possess more nodal planes in the orbital electron density distributions. The orbitals of the conformations therefore exhibit nearly identical orbitals MDs.

The orbital ratio that associated an a-symmetry orbital in the C_s conformer ($7a'$) with a b-symmetry orbital in the C_2 conformer ($5b$), via the $11a$ orbital to the C_1 transition state, is shown in greater detail in Fig. 6. The orbital electron contours in Figs. 6(a) and 6(b) reveal the relaxation of the shape (or electron density distributions) due to the changes in symmetry of the configurations. While the configurations exhibit certain similarities in orbitals $7a'$ (C_s) and $11a$ (C_1), such similarities cannot be maintained in orbital $5b$ when the C_2 conformer is formed. The orbital loses the "ring" shape in C_2 [bottom view in Fig. 6(b)], which is revealed quantitatively by orbital MDs as shown in Fig. 6(c).

The orbital MDs of set 17 ($7a''(C_s)$-$17a(C_1)$-$8b(C_2)$) are nearly identical, suggesting that this set of orbitals in their

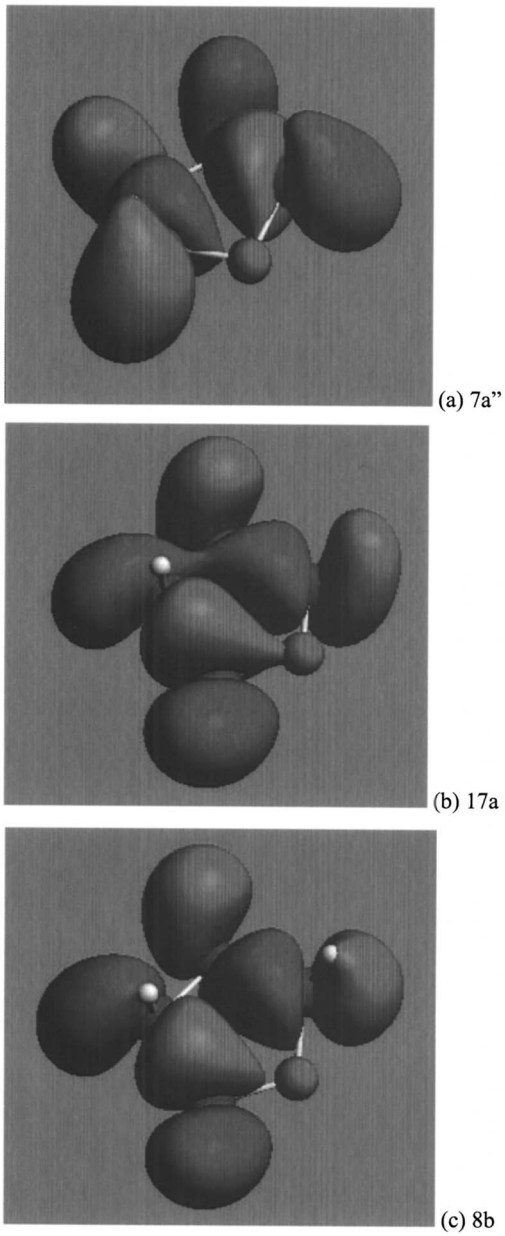

FIG. 7. The subtle differences in MO set 11 ($7a'(C_s)$-$11a(C_1)$-$6b(C_2)$)—the orbital MDs are nearly identical indicating certain similarities in their bonding mechanism.

conformations is dominated by a similar bonding mechanism of carbon $2p$ AOs. The shape of the orbital MDs suggests that the set of orbitals might be associated with AOs of higher angular momentum quantum numbers, such as d-AOs leading to a d-AO like contributions to this MO set. To explore the orbital bonding mechanism, the electron density contours of orbital set 17 are given in Fig. 7, which indicates that the orbitals are dominated by carbon $2p$-AOs in an antibonding fashion, with certain similarities to a d-AO. Therefore, this set of MOs is not dominated by d-AOs but $2p$-AOs of carbon.

MO sets in group I include three sets of frontier orbitals, MO set 20-18 ($12a'(C_s)$-$20a(C_1)$-$11a(C_2)$) HOMO (C_s); ($8a''(C_s)$-$19a(C_1)$-$9b(C_2)$), HOMO-1 (C_s), and ($11a'(C_s)$-$18a(C_1)$-$10a(C_2)$), HOMO-2 (C_s), as well as two

Downloaded 22 Jun 2009 to 136.186.1.191. Redistribution subject to AIP license or copyright; see http://jcp.aip.org/jcp/copyright.jsp

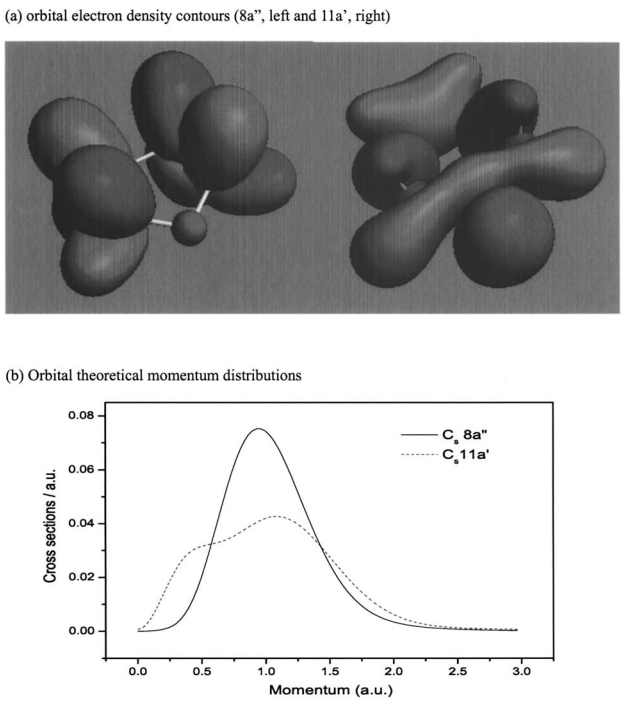

FIG. 8. The orbitals with accidental energy degeneracy: orbitals $8a'$ and $11a'$ for the C_s conformer. The electron density contours and orbital MDs for these orbitals are not the same.

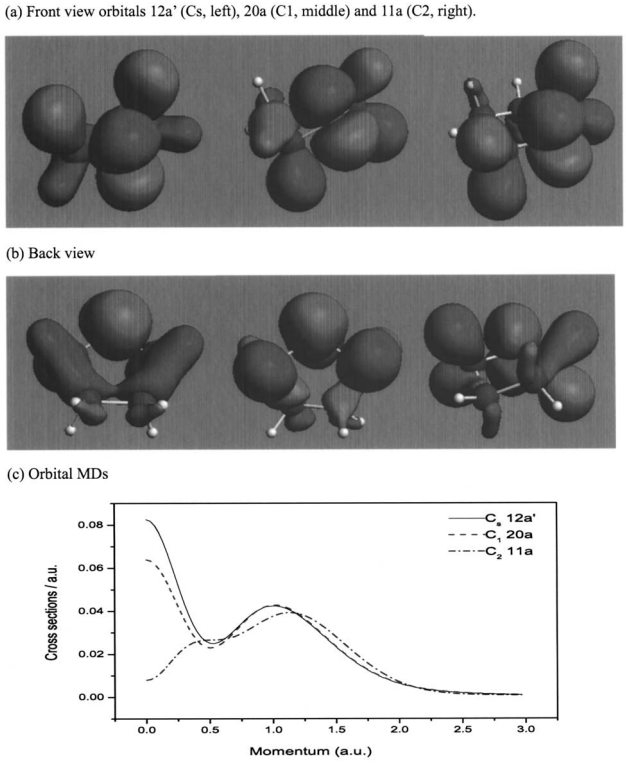

FIG. 9. Frontier orbital associations in the C_s, C_1, and C_2 conformations.

MO sets 11 and 9 of other valence orbitals, i.e., $(7a'(C_s)\text{-}11a(C_1)\text{-}5a(C_2))$ and $(4a''(C_s)\text{-}9a(C_1)\text{-}4a(C_2))$. The signature MOs differentiate the individual responses to the conformations and therefore yield important information at different stages of the pseudorotation motion of THE. As indicated in Table II (highlighted in yellow), bonding mechanisms are very different in all of these five signature MOs (MO sets 20-18, 11, and 2) or in the same set of MOs across the conformations (e.g., MO set 19 for C_s, C_1, and C_2). The orbital MDs of the inner valence orbitals, MO set 9 $(6a'(C_s)\text{-}9a(C_1)\text{-}6a(C_2))$ and MO set 11 $(7a'(C_s)\text{-}11a(C_1)\text{-}5a(C_2))$, show similarities and difference which pair C_s and C_1 but differentiate from C_2. In MO set 11, orbital $7a'$ of the C_s conformer is dominated by $C(2p)+H(1s)$, but orbital $11a(C_s)$ receives contributions from $O(2p)+H(1s)$. The bond formed by the $2p$ and $1s$ AOs exhibits similarities as manifested in their orbital MDs. However, the contribution of $C(2p)+O(2p)+H(1s)$ to the $5b$ orbital of the C_2 conformer causes a change to the orbital's MD.

The HOMO-1 and HOMO-2 ($8a''$ and $11a'$), of the C_s conformer are nearly degenerate in energy in the present calculations, indicating that energetic properties of this orbital pair may not be an ideal way to differentiate them. Their orbitals; either in position space as orbital electron density distributions or in momentum space as orbital momentum distributions, demonstrate their significantly different chemical bonding mechanisms. Figure 8 displays the HOMO-1 and HOMO-2 pair of the C_s conformer in (a) position space and (b) momentum space. In the more familiar position space, the orbital contours indicate that orbital $8a''$ receives dominant contributions from the $C(2p)+H(1s)$ AOs while the O atom is on the molecular plane. The $H(1s)$ AOs enhance the anti-π bonding mechanism which is displayed in momentum space as bell shaped orbital MDs. Orbital $11a'$ on the other hand, exhibits strong bonding in the C–O–C and HH_2-CH_2 regions as shown in Fig. 8(a) (right). The existence of certain curved nodal "planes" in their electron distributions results in the distorted orbital MDs as given in Fig. 8(b) (dashed line).

In agreement with Ref. 22 using the B3LYP/6−311++G** wave functions for the HOMOs of the C_s and C_2 conformers, the present SAOP/et-pVQZ model indeed supports the conclusion made regarding the symmetries of the HOMOs. Figure 9 (a front view and b back view) shows the HOMOs of C_s ($12a'$, left), C_1 ($20a$, middle), and HOMO-1 of C_2 ($11a$, right) conformations in order to explore how the orbitals are associated during pseudorotation. In position space, the orbital front view shows certain similarities of the configurations during different stages of the ring pseudorotation, such as the strong π-(anti)bonding in the C–O–C region. However, for this MO, perhaps it is the CH_2-CH_2 region opposite to C–O–C which contributes to the changes in their bonding characters, as demonstrated in Fig. 9(b), the back view. It is interesting that the four hydrogen atoms associated with the CH_2-CH_2 region of THF play very different roles in their bonding: in orbital $12a'$ (C_s), only a pair of the four hydrogen atoms makes small contributions to the HOMO ($12a'$) in a bowling ball shape situated on the same side of the ring. When the ring loses the symmetry plane and becomes C_1, the puckering of the ring in fact leaves only one of the four hydrogen atoms remaining unbound, which also changes the electron distributions in the CH_2-CH_2 region. As a result of the symmetry loss, the bowling ball shaped

Downloaded 22 Jun 2009 to 136.186.1.191. Redistribution subject to AIP license or copyright; see http://jcp.aip.org/jcp/copyright.jsp

hydrogen electron distribution no longer exists but the major features of the C–O–C region remain in the HOMO of the C_1 conformer.

The orbital in the C_1 conformer associated with the HOMOs of C_s and C_1 is the HOMO-1 ($11a$). Electron distributions of the C–O–C region are only slightly distorted, which is seen in Fig. 9(a) (right) for the electron density distribution and Fig. 9(d) (dash-dotted line) for orbital MDs. The apparent difference in the back view of this orbital ($11a$), again stems from the bonding of the four hydrogen atoms in the CH_2-CH_2 region. The pair of hydrogen atoms on either side of the C–C bond do not make a significant contribution to orbital $11a$ of the C_2 conformer, whereas the other hydrogen pair do; they show a sausage-shaped electron density distributions rather than the bowling ball shaped distribution as in orbital $12a'$ of the C_s conformer. The symmetry correlated orbital MDs of the conformations, in which $12a'$ and $20a$ are the HOMOs for C_s and C_1, respectively, but orbital $11a$ is the HOMO-1 for conformer C_2 in Fig. 9(c), indeed demonstrate the differences between the orbitals.

IV. CONCLUSIONS

The pseudorotation of tetrahydrofuran (THF) has been studied using molecular orbital theory. The valence spaces of three characteristic configurations, C_s, C_1, and C_2, have been investigated in position and momentum space using dual space analysis (DSA). The orbital symmetries of these conformations produced by the pseudorotation exhibit changes in point groups quite different from those produced by conformers arising from rotations around a single bond such as *n*-butane.[2,4,40] The conformers of THF represent the local minima which connect via the C_1 transition state on the PES.

Pseudorotation is a very important process to understand sugar puckering and, therefore, DNA/RNA fragments and their structures, interactions, and dynamics. The present study also demonstrates that a comprehensive understanding of the pseudorotation of THF requires multidimensional information: energy and wave function, in position space and momentum space. The THF conformations yield only subtle differences in energy, such as the total energies and the valence orbital energies. The later makes it difficult to differentiate the conformers from a number of energy dominant experiments. However, their electronic spectra (mainly due to excitation) certainly indicate that the conformers are different species as little similarities among their individual spectra are shown. However, the differences in their electronic spectra are sufficient to prove that the conformers are not the same species but insufficient to identify which spectra belongs to which conformer and the stability of each conformer in a mixture.

Orbitals are important and fundamental information to trace other molecular properties and dynamics of a species. The present work indicates the importance of combining information from position space and momentum space, that is, the importance of dual space analysis. The accidentally degenerate orbitals, $8a''$ and $11a'$ of the C_s conformer, show few similarities in their orbitals, but orbitals with subtle differences in electron distributions in space can be easily differentiated using their orbital MDs. Momentum space information provides a quantitative measurement of the orbitals which is supplementary to assist our understanding of chemical bonding mechanism associated with processes such as pseudorotation.

ACKNOWLEDGMENTS

Two of the authors (P.D. and F.W.) acknowledge the Australian Research Council (ARC) for an International Linkage Award and the Australian Partnership for Advanced Computing (APAC) for an award under the Merit Allocation Scheme on the APAC National Facility at the ANU. One of the authors (F.W.) acknowledges Ms. F. F. Chen for producing the orbital momentum distributions. Another author (J.A.S.) thanks partial financial support by MEC (Madrid, Spain) under Project No. MEC-04-CTQ-07405-C02-02. Another author (P.D.) is grateful to Professor C.E. Brion of the University of British Columbia for making available the HEMS code used to produce the MDs for this study.

[1] J. E. Kilpatrick, K. S. Pitzer, and R. Spitzer, J. Am. Chem. Soc. **69**, 2483 (1947).
[2] S. Saha, F. Wang, C. T. Falzon, and M. J. Brunger, J. Chem. Phys. **123**, 124315 (2005).
[3] F. Monnat, P. Vogel, V. M. Rayón, and J. A. Sordo, J. Org. Chem. **67**, 1882 (2002).
[4] For example, for the prototypical case of the simplest naturally occurring amino acid (glycine), see the following references: (a) P. D. Godfrey and R. D. brown, J. Am. Chem. Soc. **117**, 2019 (1995); (b) C. T. Falzon and F. Wang, J. Chem. Phys. **123**, 214307 (2005); (c) J. L. Alonso, E. J. Cocinero, A. Lesarri, M. E. Sanz, and J. C. López, Angew. Chem., Int. Ed. **45**, 3471 (2006); (d) V. Kasalová, W. D. Allen, H. F. Schaffer III, E. Czinki, and A. G. Császár, J. Comput. Chem. **28**, 1373 (2007).
[5] Y. Choi, C. George, M. J. Comin *et al.*, J. Med. Chem. **46**, 2392 (2003).
[6] (a) A. C. Legon, Chem. Rev. (Washington, D.C.) **80**, 231 (1980); (b) H. L. Strauss, Annu. Rev. Phys. Chem. **34**, 301 (1983); (c) S. SenGupta, H. P. Upadhyaya, A. Kumar, P. D. Naik, and P. Bajaj, J. Chem. Phys. **122**, 124309 (2005).
[7] V. M. Rayón and J. A. Sordo, J. Chem. Phys. **122**, 204303 (2005).
[8] D. G. Melnik, S. Gopalakrishnan, T. A. Miller, and F. C. De Lucia, J. Chem. Phys. **118**, 3589 (2003).
[9] B. Cadioli, E. Gallinella, C. Coulombeau, H. Jobic, and G. Berthier, J. Phys. Chem. **97**, 7844 (1993).
[10] E. Jawetz, in *Antiviral Chemotherapy and Prophylaxis: Basic and Clinical Pharmacology*, edited by B. G. Katzung (Applenton & Lange, Englewood Cliffs, NJ, 1992), p. 674.
[11] C. J. Cramer, *Essentials of Computational Chemistry: Theories and Models* (Wiley, Chichester, 2002).
[12] G. G. Engerholm, A. C. Luntz, W. D. Gwinn, and D. O. Harris, J. Chem. Phys. **50**, 2446 (1969).
[13] R. Meyer, J. C. Lopez, J. L. Alonso, S. Melandri, P. G. Favero, and W. Caminati, J. Chem. Phys. **111**, 7871 (1999).
[14] A. H. Mamleev, L. N. Gunderova, and R. V. Gallev, J. Struct. Chem. **42**, 365 (2001).
[15] S. J. Han and Y. K. Kang, J. Mol. Struct.: THEOCHEM **369**, 157 (1996).
[16] A. Wu and D. Cremer, Int. J. Mol. Sci. **4**, 158 (2003).
[17] J. A. Sodo, J. Chem. Phys. **114**, 1974 (2001) and references therein.
[18] T. Yang, G. Su, C. Ning, J. Deng, F. Wang, S. Zhang, X. Ren, and Y. Huang, J. Phys. Chem. A **111**, 4927 (2007).
[19] F. J. Wang, J. Phys. Chem. **107**, 10199 (2003).
[20] M. J. Frisch, G. W. Trucks, H. B. Schlegel *et al.*, GAUSSIAN 03, Revision C.02, Gaussian, Inc., Wallingford, CT, 2004.
[21] T. Kupperens, k. Vandyck, J. Van der Eycken, W. Herrebout, B. Van der Veken, and P. Bultinck, Spectrochim. Acta, Part A **67**, 402 (2007).
[22] R. F. W. Bader, J. Phys. Chem. **111**, 7966 (2007).
[23] F. Wang, P. Duffy, and D. P. Chong, in *Nanoscale interactions and their applications: Essay in Honour of IanMcCarthy*, edited by F. Wang and M. J. Brunger (Research Signpost, Kerala, India, 2007), pp. 168–181.
[24] M. Downton and F. Wang, Chem. Phys. Lett. **384**, 144 (2004).

Downloaded 22 Jun 2009 to 136.186.1.191. Redistribution subject to AIP license or copyright; see http://jcp.aip.org/jcp/copyright.jsp

[25] F. Wang and M. Downton, J. Phys. B **37**, 557 (2004).
[26] F. Wang, J. Mol. Struct.: THEOCHEM **728**, 31 (2005).
[27] F. Wang, M. Downton, and N. Kidwani, J. Theor. Comput. Chem. **4**, 247 (2005).
[28] C. T. Falzon, F. Wang, and W. Pang, J. Phys. Chem. B **110**, 9713 (2006).
[29] C. Lee, W. Yang, and R. G. Parr, Phys. Rev. B **37**, 785 (1988).
[30] A. D. Becke, J. Chem. Phys. **98**, 5648 (1993).
[31] O. V. Gritsenko, P. R. T. Schipper, and E. J. Baerends, Chem. Phys. Lett. **302**, 199 (1999).
[32] P. R. T. Schipper, O. V. Gritsenko, S. J. A. van Gisberger, and E. J. Baerends, J. Chem. Phys. **112**, 1344 (2000).
[33] A. D. F. Baerends, E. J. Austchbach, J. Brces, A. Bo, C. Boerrigter, P. M. Cavallo, and L. Chong, ADF2006.01, SCM, Vije Universiteit, Amsterdam, The Netherlands, 2005.
[34] E. Weigold and J. E. McCarthy, Rep. Prog. Phys. **54**, 789 (1991).
[35] E. Weigold and I. E. McCarthy, *Electron Momentum Spectroscopy* (Kluwer, Dordrecht/Plenum, New York, 1999).
[36] P. Duffy, D. P. Chong, M. E. Casida, and D. R. Salahub, Phys. Rev. A **50**, 4707 (1994).
[37] C. E. Brion, Int. J. Quantum Chem. **29**, 1397 (1986).
[38] P. Duffy, S. A. C. Clark, C. E. Brion, M. E. Casida, D. P. Chong, E. R. Davidson, and C. Maxwell, Chem. Phys. **165**, 183 (1992).
[39] K. B. Shakman and D. A. Mazziotti, J. Phys. Chem. A **111**, 7223 (2007).
[40] K. Kimura, S. Katsuwata, Y. Achiba, T. Yamazaki, S. Iwata, *Handbook of Hel Phtoelectron Spectra of Fundamental Organic Molecules* (Halsted, New York, 1981).
[41] J. M. Hollas, *Modern Spectroscopy*, 4th ed. (Wiley, England, 2004).
[42] A. D. Walsh, J. Chem. Soc. **1953**, 2260.
[43] F. Wang and W. N. Pang, Mol. Simul. **32**, 1173 (2007).
[44] F. Wang, M. J. Brunger, I. E. McCarthy, and D. A. Winkler, Chem. Phys. Lett. **382**, 217 (2003).

Downloaded 22 Jun 2009 to 136.186.1.191. Redistribution subject to AIP license or copyright; see http://jcp.aip.org/jcp/copyright.jsp